PHYSICAL REVIEW D **73,** 071102(R) (2006)

Branching fraction limits for B^0 decays to $\eta'\eta$, $\eta'\pi^0$ and $\eta\pi^0$

B. Aubert,[1] R. Barate,[1] D. Boutigny,[1] F. Couderc,[1] Y. Karyotakis,[1] J. P. Lees,[1] V. Poireau,[1] V. Tisserand,[1] A. Zghiche,[1] E. Grauges,[2] A. Palano,[3] M. Pappagallo,[3] J. C. Chen,[4] N. D. Qi,[4] G. Rong,[4] P. Wang,[4] Y. S. Zhu,[4] G. Eigen,[5] I. Ofte,[5] B. Stugu,[5] G. S. Abrams,[6] M. Battaglia,[6] D. S. Best,[6] D. N. Brown,[6] J. Button-Shafer,[6] R. N. Cahn,[6] E. Charles,[6] C. T. Day,[6] M. S. Gill,[6] A. V. Gritsan,[6,*] Y. Groysman,[6] R. G. Jacobsen,[6] J. A. Kadyk,[6] L. T. Kerth,[6] Yu. G. Kolomensky,[6] G. Kukartsev,[6] G. Lynch,[6] L. M. Mir,[6] P. J. Oddone,[6] T. J. Orimoto,[6] M. Pripstein,[6] N. A. Roe,[6] M. T. Ronan,[6] W. A. Wenzel,[6] M. Barrett,[7] K. E. Ford,[7] T. J. Harrison,[7] A. J. Hart,[7] C. M. Hawkes,[7] S. E. Morgan,[7] A. T. Watson,[7] M. Fritsch,[8] K. Goetzen,[8] T. Held,[8] H. Koch,[8] B. Lewandowski,[8] M. Pelizaeus,[8] K. Peters,[8] T. Schroeder,[8] M. Steinke,[8] J. T. Boyd,[9] J. P. Burke,[9] W. N. Cottingham,[9] D. Walker,[9] T. Cuhadar-Donszelmann,[10] B. G. Fulsom,[10] C. Hearty,[10] N. S. Knecht,[10] T. S. Mattison,[10] J. A. McKenna,[10] A. Khan,[11] P. Kyberd,[11] M. Saleem,[11] L. Teodorescu,[11] V. E. Blinov,[12] A. D. Bukin,[12] A. Buzykaev,[12] V. P. Druzhinin,[12] V. B. Golubev,[12] A. P. Onuchin,[12] S. I. Serednyakov,[12] Yu. I. Skovpen,[12] E. P. Solodov,[12] K. Yu Todyshev,[12] M. Bondioli,[13] M. Bruinsma,[13] M. Chao,[13] S. Curry,[13] I. Eschrich,[13] D. Kirkby,[13] A. J. Lankford,[13] P. Lund,[13] M. Mandelkern,[13] R. K. Mommsen,[13] W. Roethel,[13] D. P. Stoker,[13] S. Abachi,[14] C. Buchanan,[14] S. D. Foulkes,[15] J. W. Gary,[15] O. Long,[15] B. C. Shen,[15] K. Wang,[15] L. Zhang,[15] D. del Re,[16] H. K. Hadavand,[16] E. J. Hill,[16] H. P. Paar,[16] S. Rahatlou,[16] V. Sharma,[16] J. W. Berryhill,[17] C. Campagnari,[17] A. Cunha,[17] B. Dahmes,[17] T. M. Hong,[17] J. D. Richman,[17] T. W. Beck,[18] A. M. Eisner,[18] C. J. Flacco,[18] C. A. Heusch,[18] J. Kroseberg,[18] W. S. Lockman,[18] G. Nesom,[18] T. Schalk,[18] B. A. Schumm,[18] A. Seiden,[18] P. Spradlin,[18] D. C. Williams,[18] M. G. Wilson,[18] J. Albert,[19] E. Chen,[19] G. P. Dubois-Felsmann,[19] A. Dvoretskii,[19] D. G. Hitlin,[19] I. Narsky,[19] T. Piatenko,[19] F. C. Porter,[19] A. Ryd,[19] A. Samuel,[19] R. Andreassen,[20] G. Mancinelli,[20] B. T. Meadows,[20] M. D. Sokoloff,[20] E. A. Antillon,[21] F. Blanc,[21] P. C. Bloom,[21] S. Chen,[21] W. T. Ford,[21] J. F. Hirschauer,[21] A. Kreisel,[21] U. Nauenberg,[21] A. Olivas,[21] W. O. Ruddick,[21] J. G. Smith,[21] K. A. Ulmer,[21] S. R. Wagner,[21] J. Zhang,[21] A. Chen,[22] E. A. Eckhart,[22] A. Soffer,[22] W. H. Toki,[22] R. J. Wilson,[22] F. Winklmeier,[22] Q. Zeng,[22] D. D. Altenburg,[23] E. Feltresi,[23] A. Hauke,[23] H. Jasper,[23] B. Spaan,[23] T. Brandt,[24] V. Klose,[24] H. M. Lacker,[24] R. Nogowski,[24] A. Petzold,[24] J. Schubert,[24] K. R. Schubert,[24] R. Schwierz,[24] J. E. Sundermann,[24] A. Volk,[24] D. Bernard,[25] G. R. Bonneaud,[25] P. Grenier,[25,†] E. Latour,[25] Ch. Thiebaux,[25] M. Verderi,[25] D. J. Bard,[26] P. J. Clark,[26] W. Gradl,[26] F. Muheim,[26] S. Playfer,[26] Y. Xie,[26] M. Andreotti,[27] D. Bettoni,[27] C. Bozzi,[27] R. Calabrese,[27] G. Cibinetto,[27] E. Luppi,[27] M. Negrini,[27] L. Piemontese,[27] F. Anulli,[28] R. Baldini-Ferroli,[28] A. Calcaterra,[28] R. de Sangro,[28] G. Finocchiaro,[28] S. Pacetti,[28] P. Patteri,[28] I. M. Peruzzi,[28,‡] M. Piccolo,[28] A. Zallo,[28] A. Buzzo,[29] R. Capra,[29] R. Contri,[29] M. Lo Vetere,[29] M. M. Macri,[29] M. R. Monge,[29] S. Passaggio,[29] C. Patrignani,[29] E. Robutti,[29] A. Santroni,[29] S. Tosi,[29] G. Brandenburg,[30] K. S. Chaisanguanthum,[30] M. Morii,[30] J. Wu,[30] R. S. Dubitzky,[31] J. Marks,[31] S. Schenk,[31] U. Uwer,[31] W. Bhimji,[32] D. A. Bowerman,[32] P. D. Dauncey,[32] U. Egede,[32] R. L. Flack,[32] J. R. Gaillard,[32] J. A. Nash,[32] M. B. Nikolich,[32] W. Panduro Vazquez,[32] X. Chai,[33] M. J. Charles,[33] W. F. Mader,[33] U. Mallik,[33] V. Ziegler,[33] J. Cochran,[34] H. B. Crawley,[34] L. Dong,[34] V. Eyges,[34] W. T. Meyer,[34] S. Prell,[34] E. I. Rosenberg,[34] A. E. Rubin,[34] G. Schott,[35] N. Arnaud,[36] M. Davier,[36] G. Grosdidier,[36] A. Höcker,[36] F. Le Diberder,[36] V. Lepeltier,[36] A. M. Lutz,[36] A. Oyanguren,[36] T. C. Petersen,[36] S. Pruvot,[36] S. Rodier,[36] P. Roudeau,[36] M. H. Schune,[36] A. Stocchi,[36] W. F. Wang,[36] G. Wormser,[36] C. H. Cheng,[37] D. J. Lange,[37] D. M. Wright,[37] C. A. Chavez,[38] I. J. Forster,[38] J. R. Fry,[38] E. Gabathuler,[38] R. Gamet,[38] K. A. George,[38] D. E. Hutchcroft,[38] D. J. Payne,[38] K. C. Schofield,[38] C. Touramanis,[38] A. J. Bevan,[39] F. Di Lodovico,[39] W. Menges,[39] R. Sacco,[39] C. L. Brown,[40] G. Cowan,[40] H. U. Flaecher,[40] D. A. Hopkins,[40] P. S. Jackson,[40] T. R. McMahon,[40] S. Ricciardi,[40] F. Salvatore,[40] D. N. Brown,[41] C. L. Davis,[41] J. Allison,[42] N. R. Barlow,[42] R. J. Barlow,[42] Y. M. Chia,[42] C. L. Edgar,[42] M. P. Kelly,[42] G. D. Lafferty,[42] M. T. Naisbit,[42] J. C. Williams,[42] J. I. Yi,[42] C. Chen,[43] W. D. Hulsbergen,[43] A. Jawahery,[43] D. Kovalskyi,[43] C. K. Lae,[43] D. A. Roberts,[43] G. Simi,[43] G. Blaylock,[44] C. Dallapiccola,[44] S. S. Hertzbach,[44] X. Li,[44] T. B. Moore,[44] S. Saremi,[44] H. Staengle,[44] S. Y. Willocq,[44] R. Cowan,[45] K. Koeneke,[45] G. Sciolla,[45] S. J. Sekula,[45] M. Spitznagel,[45] F. Taylor,[45] R. K. Yamamoto,[45] H. Kim,[46] P. M. Patel,[46] C. T. Potter,[46] S. H. Robertson,[46] A. Lazzaro,[47] V. Lombardo,[47] F. Palombo,[47] J. M. Bauer,[48] L. Cremaldi,[48] V. Eschenburg,[48] R. Godang,[48] R. Kroeger,[48] J. Reidy,[48] D. A. Sanders,[48] D. J. Summers,[48] H. W. Zhao,[48] S. Brunet,[49] D. Côté,[49] M. Simard,[49] P. Taras,[49] F. B. Viaud,[49] H. Nicholson,[50] N. Cavallo,[51,§] G. De Nardo,[51] F. Fabozzi,[51,§] C. Gatto,[51] L. Lista,[51] D. Monorchio,[51] D. Piccolo,[51] C. Sciacca,[51] M. Baak,[52] H. Bulten,[52] G. Raven,[52] H. L. Snoek,[52] C. P. Jessop,[53] J. M. LoSecco,[53] T. Allmendinger,[54] G. Benelli,[54] K. K. Gan,[54] K. Honscheid,[54] D. Hufnagel,[54] P. D. Jackson,[54] H. Kagan,[54] R. Kass,[54] T. Pulliam,[54] A. M. Rahimi,[54] R. Ter-Antonyan,[54] Q. K. Wong,[54] N. L. Blount,[55] J. Brau,[55] R. Frey,[55] O. Igonkina,[55] M. Lu,[55] R. Rahmat,[55] N. B. Sinev,[55] D. Strom,[55] J. Strube,[55] E. Torrence,[55] F. Galeazzi,[56] A. Gaz,[56] M. Margoni,[56] M. Morandin,[56] A. Pompili,[56] M. Posocco,[56] M. Rotondo,[56]

F. Simonetto,[56] R. Stroili,[56] C. Voci,[56] M. Benayoun,[57] J. Chauveau,[57] P. David,[57] L. Del Buono,[57] Ch. de la Vaissière,[57] O. Hamon,[57] B. L. Hartfiel,[57] M. J. J. John,[57] Ph. Leruste,[57] J. Malclès,[57] J. Ocariz,[57] L. Roos,[57] G. Therin,[57] P. K. Behera,[58] L. Gladney,[58] J. Panetta,[58] M. Biasini,[59] R. Covarelli,[59] M. Pioppi,[59] C. Angelini,[60] G. Batignani,[60] S. Bettarini,[60] F. Bucci,[60] G. Calderini,[60] M. Carpinelli,[60] R. Cenci,[60] F. Forti,[60] M. A. Giorgi,[60] A. Lusiani,[60] G. Marchiori,[60] M. A. Mazur,[60] M. Morganti,[60] N. Neri,[60] E. Paoloni,[60] M. Rama,[60] G. Rizzo,[60] J. Walsh,[60] M. Haire,[61] D. Judd,[61] D. E. Wagoner,[61] J. Biesiada,[62] N. Danielson,[62] P. Elmer,[62] Y. P. Lau,[62] C. Lu,[62] J. Olsen,[62] A. J. S. Smith,[62] A. V. Telnov,[62] F. Bellini,[63] G. Cavoto,[63] A. D'Orazio,[63] E. Di Marco,[63] R. Faccini,[63] F. Ferrarotto,[63] F. Ferroni,[63] M. Gaspero,[63] L. Li Gioi,[63] M. A. Mazzoni,[63] S. Morganti,[63] G. Piredda,[63] F. Polci,[63] F. Safai Tehrani,[63] C. Voena,[63] H. Schröder,[64] R. Waldi,[64] T. Adye,[65] N. De Groot,[65] B. Franek,[65] E. O. Olaiya,[65] F. F. Wilson,[65] S. Emery,[66] A. Gaidot,[66] S. F. Ganzhur,[66] G. Hamel de Monchenault,[66] W. Kozanecki,[66] M. Legendre,[66] B. Mayer,[66] G. Vasseur,[66] Ch. Yèche,[66] M. Zito,[66] W. Park,[67] M. V. Purohit,[67] A. W. Weidemann,[67] J. R. Wilson,[67] M. T. Allen,[68] D. Aston,[68] R. Bartoldus,[68] P. Bechtle,[68] N. Berger,[68] A. M. Boyarski,[68] R. Claus,[68] J. P. Coleman,[68] M. R. Convery,[68] M. Cristinziani,[68] J. C. Dingfelder,[68] D. Dong,[68] J. Dorfan,[68] D. Dujmic,[68] W. Dunwoodie,[68] R. C. Field,[68] T. Glanzman,[68] S. J. Gowdy,[68] V. Halyo,[68] C. Hast,[68] T. Hryn'ova,[68] W. R. Innes,[68] M. H. Kelsey,[68] P. Kim,[68] M. L. Kocian,[68] D. W. G. S. Leith,[68] J. Libby,[68] S. Luitz,[68] V. Luth,[68] H. L. Lynch,[68] D. B. MacFarlane,[68] H. Marsiske,[68] R. Messner,[68] D. R. Muller,[68] C. P. O'Grady,[68] V. E. Ozcan,[68] A. Perazzo,[68] M. Perl,[68] B. N. Ratcliff,[68] A. Roodman,[68] A. A. Salnikov,[68] R. H. Schindler,[68] J. Schwiening,[68] A. Snyder,[68] J. Stelzer,[68] D. Su,[68] M. K. Sullivan,[68] K. Suzuki,[68] S. K. Swain,[68] J. M. Thompson,[68] J. Va'vra,[68] N. van Bakel,[68] M. Weaver,[68] A. J. R. Weinstein,[68] W. J. Wisniewski,[68] M. Wittgen,[68] D. H. Wright,[68] A. K. Yarritu,[68] K. Yi,[68] C. C. Young,[68] P. R. Burchat,[69] A. J. Edwards,[69] S. A. Majewski,[69] B. A. Petersen,[69] C. Roat,[69] L. Wilden,[69] S. Ahmed,[70] M. S. Alam,[70] R. Bula,[70] J. A. Ernst,[70] V. Jain,[70] B. Pan,[70] M. A. Saeed,[70] F. R. Wappler,[70] S. B. Zain,[70] W. Bugg,[71] M. Krishnamurthy,[71] S. M. Spanier,[71] R. Eckmann,[72] J. L. Ritchie,[72] A. Satpathy,[72] R. F. Schwitters,[72] J. M. Izen,[73] I. Kitayama,[73] X. C. Lou,[73] S. Ye,[73] F. Bianchi,[74] M. Bona,[74] F. Gallo,[74] D. Gamba,[74] M. Bomben,[75] L. Bosisio,[75] C. Cartaro,[75] F. Cossutti,[75] G. Della Ricca,[75] S. Dittongo,[75] S. Grancagnolo,[75] L. Lanceri,[75] L. Vitale,[75] V. Azzolini,[76] F. Martinez-Vidal,[76] R. S. Panvini,[77,‖] Sw. Banerjee,[78] B. Bhuyan,[78] C. M. Brown,[78] D. Fortin,[78] K. Hamano,[78] R. Kowalewski,[78] I. M. Nugent,[78] J. M. Roney,[78] R. J. Sobie,[78] J. J. Back,[79] P. F. Harrison,[79] T. E. Latham,[79] G. B. Mohanty,[79] H. R. Band,[80] X. Chen,[80] B. Cheng,[80] S. Dasu,[80] M. Datta,[80] A. M. Eichenbaum,[80] K. T. Flood,[80] M. T. Graham,[80] J. J. Hollar,[80] J. R. Johnson,[80] P. E. Kutter,[80] H. Li,[80] R. Liu,[80] B. Mellado,[80] A. Mihalyi,[80] A. K. Mohapatra,[80] Y. Pan,[80] M. Pierini,[80] R. Prepost,[80] P. Tan,[80] S. L. Wu,[80] Z. Yu,[80] and H. Neal[81]

(*BABAR* Collaboration)

[1]*Laboratoire de Physique des Particules, F-74941 Annecy-le-Vieux, France*
[2]*Universitat de Barcelona, Fac. Fisica Dept. ECM, Avda Diagonal 647, 6a planta, E-08028 Barcelona, Spain*
[3]*Dipartimento di Fisica and INFN, Università di Bari, I-70126 Bari, Italy*
[4]*Institute of High Energy Physics, Beijing 100039, China*
[5]*University of Bergen, Institute of Physics, N-5007 Bergen, Norway*
[6]*Lawrence Berkeley National Laboratory and University of California, Berkeley, California 94720, USA*
[7]*University of Birmingham, Birmingham, B15 2TT, United Kingdom*
[8]*Ruhr Universität Bochum, Institut für Experimentalphysik 1, D-44780 Bochum, Germany*
[9]*University of Bristol, Bristol BS8 1TL, United Kingdom*
[10]*University of British Columbia, Vancouver, British Columbia, Canada V6T 1Z1*
[11]*Brunel University, Uxbridge, Middlesex UB8 3PH, United Kingdom*
[12]*Budker Institute of Nuclear Physics, Novosibirsk 630090, Russia*
[13]*University of California at Irvine, Irvine, California 92697, USA*
[14]*University of California at Los Angeles, Los Angeles, California 90024, USA*
[15]*University of California at Riverside, Riverside, California 92521, USA*
[16]*University of California at San Diego, La Jolla, California 92093, USA*
[17]*University of California at Santa Barbara, Santa Barbara, California 93106, USA*
[18]*University of California at Santa Cruz, Institute for Particle Physics, Santa Cruz, California 95064, USA*
[19]*California Institute of Technology, Pasadena, California 91125, USA*
[20]*University of Cincinnati, Cincinnati, Ohio 45221, USA*
[21]*University of Colorado, Boulder, Colorado 80309, USA*
[22]*Colorado State University, Fort Collins, Colorado 80523, USA*
[23]*Universität Dortmund, Institut für Physik, D-44221 Dortmund, Germany*
[24]*Technische Universität Dresden, Institut für Kern- und Teilchenphysik, D-01062 Dresden, Germany*

[25]*Ecole Polytechnique, LLR, F-91128 Palaiseau, France*
[26]*University of Edinburgh, Edinburgh EH9 3JZ, United Kingdom*
[27]*Università di Ferrara, Dipartimento di Fisica and INFN, I-44100 Ferrara, Italy*
[28]*Laboratori Nazionali di Frascati dell'INFN, I-00044 Frascati, Italy*
[29]*Università di Genova, Dipartimento di Fisica and INFN, I-16146 Genova, Italy*
[30]*Harvard University, Cambridge, Massachusetts 02138, USA*
[31]*Universität Heidelberg, Physikalisches Institut, Philosophenweg 12, D-69120 Heidelberg, Germany*
[32]*Imperial College London, London, SW7 2AZ, United Kingdom*
[33]*University of Iowa, Iowa City, Iowa 52242, USA*
[34]*Iowa State University, Ames, Iowa 50011-3160, USA*
[35]*Universität Karlsruhe, Institut für Experimentelle Kernphysik, D-76021 Karlsruhe, Germany*
[36]*Laboratoire de l'Accélérateur Linéaire, IN2P3-CNRS et Université Paris-Sud 11, Centre Scientifique d'Orsay, B.P. 34, F-91898 ORSAY Cedex, France*
[37]*Lawrence Livermore National Laboratory, Livermore, California 94550, USA*
[38]*University of Liverpool, Liverpool L69 7ZE, United Kingdom*
[39]*Queen Mary, University of London, E1 4NS, United Kingdom*
[40]*University of London, Royal Holloway and Bedford New College, Egham, Surrey TW20 0EX, United Kingdom*
[41]*University of Louisville, Louisville, Kentucky 40292, USA*
[42]*University of Manchester, Manchester M13 9PL, United Kingdom*
[43]*University of Maryland, College Park, Maryland 20742, USA*
[44]*University of Massachusetts, Amherst, Massachusetts 01003, USA*
[45]*Massachusetts Institute of Technology, Laboratory for Nuclear Science, Cambridge, Massachusetts 02139, USA*
[46]*McGill University, Montréal, Québec, Canada H3A 2T8*
[47]*Università di Milano, Dipartimento di Fisica and INFN, I-20133 Milano, Italy*
[48]*University of Mississippi, University, Mississippi 38677, USA*
[49]*Université de Montréal, Physique des Particules, Montréal, Québec, Canada H3C 3J7*
[50]*Mount Holyoke College, South Hadley, Massachusetts 01075, USA*
[51]*Università di Napoli Federico II, Dipartimento di Scienze Fisiche and INFN, I-80126, Napoli, Italy*
[52]*NIKHEF, National Institute for Nuclear Physics and High Energy Physics, NL-1009 DB Amsterdam, The Netherlands*
[53]*University of Notre Dame, Notre Dame, Indiana 46556, USA*
[54]*Ohio State University, Columbus, Ohio 43210, USA*
[55]*University of Oregon, Eugene, Oregon 97403, USA*
[56]*Università di Padova, Dipartimento di Fisica and INFN, I-35131 Padova, Italy*
[57]*Universités Paris VI et VII, Laboratoire de Physique Nucléaire et de Hautes Energies, F-75252 Paris, France*
[58]*University of Pennsylvania, Philadelphia, Pennsylvania 19104, USA*
[59]*Università di Perugia, Dipartimento di Fisica and INFN, I-06100 Perugia, Italy*
[60]*Università di Pisa, Dipartimento di Fisica, Scuola Normale Superiore and INFN, I-56127 Pisa, Italy*
[61]*Prairie View A&M University, Prairie View, Texas 77446, USA*
[62]*Princeton University, Princeton, New Jersey 08544, USA*
[63]*Università di Roma La Sapienza, Dipartimento di Fisica and INFN, I-00185 Roma, Italy*
[64]*Universität Rostock, D-18051 Rostock, Germany*
[65]*Rutherford Appleton Laboratory, Chilton, Didcot, Oxon, OX11 0QX, United Kingdom*
[66]*DSM/Dapnia, CEA/Saclay, F-91191 Gif-sur-Yvette, France*
[67]*University of South Carolina, Columbia, South Carolina 29208, USA*
[68]*Stanford Linear Accelerator Center, Stanford, California 94309, USA*
[69]*Stanford University, Stanford, California 94305-4060, USA*
[70]*State University of New York, Albany, New York 12222, USA*
[71]*University of Tennessee, Knoxville, Tennessee 37996, USA*
[72]*University of Texas at Austin, Austin, Texas 78712, USA*
[73]*University of Texas at Dallas, Richardson, Texas 75083, USA*
[74]*Università di Torino, Dipartimento di Fisica Sperimentale and INFN, I-10125 Torino, Italy*
[75]*Università di Trieste, Dipartimento di Fisica and INFN, I-34127 Trieste, Italy*
[76]*IFIC, Universitat de Valencia-CSIC, E-46071 Valencia, Spain*
[77]*Vanderbilt University, Nashville, Tennessee 37235, USA*

[*]Also with the Johns Hopkins University, Baltimore, MD 21218, USA
[†]Also at Laboratoire de Physique Corpusculaire, Clermont-Ferrand, France
[‡]Also with Università di Perugia, Dipartimento di Fisica, Perugia, Italy
[§]Also with Università della Basilicata, Potenza, Italy
[‖]Deceased

[78]*University of Victoria, Victoria, British Columbia, Canada V8W 3P6*
[79]*Department of Physics, University of Warwick, Coventry CV4 7AL, United Kingdom*
[80]*University of Wisconsin, Madison, Wisconsin 53706, USA*
[81]*Yale University, New Haven, Connecticut 06511, USA*
(Received 7 March 2006; published 12 April 2006)

We describe searches for decays to two-body charmless final states $\eta'\eta$, $\eta'\pi^0$ and $\eta\pi^0$ of B^0 mesons produced in e^+e^- annihilation. The data, collected with the *BABAR* detector at the Stanford Linear Accelerator Center, represent 232×10^6 produced $B\bar{B}$ pairs. The results for branching fractions are, in units of 10^{-6} (upper limits at 90% C.L.): $\mathcal{B}(B^0\to\eta'\eta)=0.2^{+0.7}_{-0.5}\pm0.4(<1.7)$, $\mathcal{B}(B^0\to\eta\pi^0)=0.6^{+0.5}_{-0.4}\pm0.1(<1.3)$, and $\mathcal{B}(B^0\to\eta'\pi^0)=0.8^{+0.8}_{-0.6}\pm0.1(<2.1)$. The first error quoted is statistical and the second systematic.

DOI: 10.1103/PhysRevD.73.071102 PACS numbers: 13.25.Hw, 11.30.Er, 12.15.Hh

We present the results of searches for neutral B meson decays to $\eta'\eta$, $\eta\pi^0$ and $\eta'\pi^0$, with a data sample expanded by about a factor of 2.6 over the one used for our previous measurements [1,2]. In the standard model (SM) the processes that contribute to these decays are described by color-suppressed tree and one-loop gluonic, electroweak or flavor-singlet penguin amplitudes. For $B^0\to\eta'\pi^0$ and $B^0\to\eta\pi^0$ the color-suppressed tree diagram is also suppressed by approximate cancellation between the amplitudes for the π^0 and for the isoscalar meson to contain the spectator quark, resulting from the mesons' isospin couplings to the quarks. Estimates of the branching fractions for these modes have been obtained from calculations based on QCD factorization [3,4], perturbative QCD (for $B^0\to\eta^{(\prime)}\pi^0$) [5], soft collinear effective theory [6], and flavor-SU(3) symmetry [7,8]. The expectations lie in the approximate ranges 0.2–1.0×10^{-6} for $B^0\to\eta^{(\prime)}\pi^0$, and 0.3–2×10^{-6} for $B^0\to\eta'\eta$.

These decays are also of interest in constraining the expected value of the time-dependent CP-violation asymmetry parameter S_f in the decay with $f=\eta' K^0_S$ [7,9,10]. The leading-order SM calculation gives the equality $S_{\eta' K^0_S}=S_{J/\psi K^0_S}$, where the latter has been precisely measured [11], and equals $\sin2\beta$ in the SM. The CP asymmetry in the charmless modes is sensitive to contributions from new physics, but also to contamination from subleading SM amplitudes. The most stringent constraint on such contamination in $S_{\eta' K^0_S}$ comes from the measured branching fractions of the three decay modes studied in this paper [7,9,10]. Recently it has also been suggested [12,13] that $B^0\to\eta'\pi^0$ and $B^0\to\eta\pi^0$ can be used to constrain the contribution from isospin-breaking effects on the value of $\sin2\alpha$ in $B^0\to\pi^+\pi^-$ decays.

The results presented here are based on data collected with the *BABAR* detector [14] at the PEP-II asymmetric e^+e^- collider [15] located at the Stanford Linear Accelerator Center. An integrated luminosity of 211 fb^{-1}, corresponding to $232\times10^6\,B\bar{B}$ pairs, was recorded at the $\Upsilon(4S)$ resonance (center-of-mass energy $\sqrt{s}=10.58$ GeV).

Charged particles from the e^+e^- interactions are detected, and their momenta measured, by a combination of five layers of double-sided silicon microstrip detectors and a 40-layer drift chamber, both operating in the 1.5 T magnetic field of a superconducting solenoid. Photons and electrons are identified with a CsI(Tl) electromagnetic calorimeter (EMC). Further charged particle identification (PID) is provided by the average energy loss (dE/dx) in the tracking devices and by an internally reflecting ring imaging Cherenkov detector (DIRC) covering the central region.

We establish the event selection criteria with the aid of a detailed Monte Carlo (MC) simulation of the B production and decay sequences, and of the detector response [16]. These criteria are designed to retain signal events with high efficiency. Applied to the data, they result in a sample much larger than the expected signal, but with well-characterized backgrounds. We extract the signal yields from this sample with a maximum likelihood (ML) fit.

The B-daughter candidates are reconstructed through their decays $\pi^0\to\gamma\gamma$, $\eta\to\gamma\gamma$ ($\eta_{\gamma\gamma}$), $\eta\to\pi^+\pi^-\pi^0$ ($\eta_{3\pi}$), $\eta'\to\eta_{\gamma\gamma}\pi^+\pi^-$ ($\eta'_{\eta\pi\pi}$), and additionally for $\eta'\eta$ modes, $\eta'\to\rho^0\gamma$ ($\eta'_{\rho\gamma}$), where $\rho^0\to\pi^+\pi^-$. Table I lists the requirements on the invariant mass of these particles' final states. Secondary charged pions in η' and η candidates are rejected if classified as protons, kaons, or electrons by their DIRC, dE/dx, and EMC PID signatures.

We reconstruct the B-meson candidate by combining the four-momenta of a pair of daughter mesons, with a vertex

TABLE I. Selection requirements on the invariant masses of resonances and the laboratory energies of photons from their decay.

State	Invariant mass (MeV)	$E(\gamma)$ (MeV)
π^0	$120<m(\gamma\gamma)<150$	>50
$\eta_{\gamma\gamma}$	$490<m(\gamma\gamma)<600$	>100
$\eta_{3\pi}$	$520<m(\pi^+\pi^-\pi^0)<570$	>30
$\eta'_{\eta\pi\pi}$	$910<m(\pi^+\pi^-\eta)<1000$	>100
$\eta'_{\rho\gamma}$	$910<m(\pi^+\pi^-\gamma)<1000$	>200
ρ^0	$510<m(\pi^+\pi^-)<1000$	-

constraint if the ultimate final state includes at least two charged particles. Since the natural widths of the η, η', and π^0 are much smaller than the resolution, we also constrain their masses to nominal values [17] in the fit of the B candidate. From the kinematics of $\Upsilon(4S)$ decay we determine the energy-substituted mass $m_{\rm ES} = [\frac{1}{4}s - \mathbf{p}_B^2]^{1/2}$ and energy difference $\Delta E = E_B - \frac{1}{2}\sqrt{s}$, where $(E_B, \mathbf{p}_B)$ is the B-meson 4-momentum vector, and all values are expressed in the $\Upsilon(4S)$ frame. The resolution in $m_{\rm ES}$ is 3.0 MeV and in ΔE is 24–50 MeV, depending on the decay mode. We require $5.25\ {\rm GeV} < m_{\rm ES} < 5.29\ {\rm GeV}$ and $|\Delta E| < 0.3$ GeV (< 0.2 GeV for $\eta'\eta$).

Backgrounds arise primarily from random combinations of particles in continuum $e^+e^- \to q\bar{q}$ events ($q = u, d, s, c$). We reduce these with requirements on the angle $\theta_{\rm T}$ between the thrust axis of the B candidate in the $\Upsilon(4S)$ frame and that of the rest of the charged tracks and neutral calorimeter clusters in the event. The distribution is sharply peaked near $|\cos\theta_{\rm T}| = 1$ for $q\bar{q}$ jet pairs, and nearly uniform for B-meson decays. The requirement, which optimizes the expected signal yield relative to its background-dominated statistical error, is $|\cos\theta_{\rm T}| <$ 0.7–0.9 depending on the mode.

In the ML fit we discriminate further against $q\bar{q}$ background with a Fisher discriminant $\mathcal{F}$ that combines several variables which characterize the energy flow in the event [1]. It provides about 1 standard deviation of separation between B decay events and combinatorial background [see Fig. 1(d)].

We also impose restrictions on decay angles to exclude the most asymmetric decays where soft-particle backgrounds concentrate and the acceptance changes rapidly. We define the decay angle $\theta^k_{\rm dec}$ for a meson k as the angle between the momenta of a daughter particle and the meson's parent, measured in the meson's rest frame. We require for the $\eta'_{\rho\gamma}$ decays $|\cos\theta^\rho_{\rm dec}| < 0.9$ and for $\eta^{(\prime)}\pi^0 |\cos\theta^{\pi^0}_{\rm dec}| < 0.95$. For $B^0 \to \eta'_{\rho\gamma}\eta_{\gamma\gamma}$ the requirement is $|\cos\theta^\eta_{\rm dec}| < 0.86$ to suppress the background $B \to K^*\gamma$.

The average number of candidates found per selected event is in the range 1.06–1.23, depending on the final state. We choose the candidate with the smallest value of a χ^2 constructed from the deviations from expected values of one or more of the daughter resonance masses. From the simulation we find that this algorithm selects the correct-combination candidate in about two thirds of the events containing multiple candidates, and that it induces negligible bias.

We obtain yields for each channel from a maximum likelihood fit with the input observables ΔE, $m_{\rm ES}$, $\mathcal{F}$, and $m_{1,(2)}$, the daughter invariant mass spectrum of the η and/or η' candidate. The selected sample sizes are given in the second column of Table II. Besides any signal events they contain $q\bar{q}$ (dominant) and $B\bar{B}$ with $b \to c$ combinatorial background, and a fraction that we estimate from the simulation to be less than 0.2% of feed-across from other charmless $B\bar{B}$ modes. The latter events have ultimate final states different from the signal, but with similar kinematics so that broad peaks near those of the signal appear in some observables, requiring a separate component in the probability density function (PDF). The likelihood function is

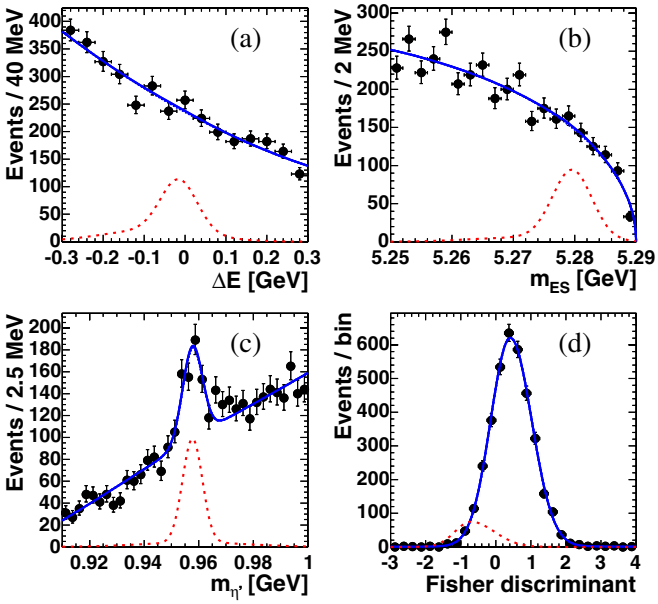

FIG. 1 (color online). Plots of the $B^0 \to \eta'_{\eta\pi\pi}\pi^0$ data distribution projected on each of the fit variables: (a) ΔE, (b) $m_{\rm ES}$, (c) η' mass, and (d) $\mathcal{F}$. The solid line represents the result of the fit, and the dashed line the background contribution. (The absence of signal here nearly hides the dashed curve.) The dotted line illustrates the expected shape for signal, with a normalization, chosen for clarity, that corresponds to a branching fraction of 50×10^{-6}.

$$\mathcal{L} = \exp\left(-\sum_j Y_j\right) \times \prod_i^N \sum_j Y_j \mathcal{P}_j(m_{\rm ES}{}^i)\mathcal{P}_j(\Delta E^i)\mathcal{P}_j(\mathcal{F}^i)\mathcal{P}_j(m_1^i) \times [\mathcal{P}_j(m_2^i)], \quad (1)$$

where N is the number of events in the sample, and for each component j, Y_j is the yield of events and $\mathcal{P}_j(x^i)$ the PDF for observable x in event i. For the modes $B^0 \to \eta'_{\eta\pi\pi}\eta$ we found no need for the $B\bar{B}$ background component. The factored form of the PDF indicated in Eq. (1) is a good approximation, particularly for the combinatorial $q\bar{q}$ component, since correlations among observables measured in the data (dominantly this component) are small. Distortions of the fit results caused by this approximation are measured in simulation and included in the bias corrections and systematic errors discussed below.

We determine the PDFs for the signal and $B\bar{B}$ background components from fits to MC data. We calibrate the

TABLE II. Number of events N in the sample, fitted signal yield Y_S in events (ev.), measured bias, detection efficiency ϵ, daughter branching fraction product ($\prod \mathcal{B}_i$), and measured branching fraction $\mathcal{B}$ for each decay chain, and for the combined measurements the significance $\mathcal{S}$ (with systematic uncertainties included), branching fraction with statistical and systematic error, and in parentheses the 90% C.L. upper limits. The number of produced $B\bar{B}$ pairs is $(231.8 \pm 2.6) \times 10^6$.

Mode	N (ev.)	Y_S (ev.)	Bias (ev.)	ϵ (%)	$\prod \mathcal{B}_i$ (%)	$\mathcal{S}$ (σ)	$\mathcal{B}$ (10^{-6})
$\eta'_{\eta\pi\pi}\eta_{3\pi}$	539	$2.0^{+3.1}_{-2.0}$	1.9 ± 1.0	13.8	3.95	$\cdots$	$0.1^{+2.4}_{-1.6}$
$\eta'_{\eta\pi\pi}\eta_{\gamma\gamma}$	1448	$2.1^{+3.5}_{-2.2}$	0.7 ± 0.4	22.3	6.89	$\cdots$	$0.4^{+1.0}_{-0.6}$
$\eta'_{\rho\gamma}\eta_{3\pi}$	8268	$-8.6^{+8.7}_{-7.0}$	0.0 ± 0.4	14.9	6.67	$\cdots$	$-3.8^{+3.8}_{-3.0}$
$\eta'_{\rho\gamma}\eta_{\gamma\gamma}$	16861	$1.5^{+10.5}_{-8.5}$	0.0 ± 0.5	21.8	11.63	$\cdots$	$0.2^{+1.8}_{-1.4}$
$\boldsymbol{\eta'\eta}$	$\cdots$	$\cdots$	$\cdots$	$\cdots$	$\cdots$	**0.4**	$\mathbf{0.2^{+0.7}_{-0.5} \pm 0.4}$ **(** $\mathbf{< 1.7}$**)**
$\eta_{3\pi}\pi^0$	2334	$10.3^{+8.6}_{-6.7}$	1.2 ± 0.7	16.3	22.6	$\cdots$	$1.1^{+1.0}_{-0.8}$
$\eta_{\gamma\gamma}\pi^0$	5493	$6.5^{+11.5}_{-9.6}$	1.2 ± 0.8	20.7	39.4	$\cdots$	$0.3^{+0.6}_{-0.5}$
$\boldsymbol{\eta\pi^0}$	$\cdots$	$\cdots$	$\cdots$	$\cdots$	$\cdots$	**1.3**	$\mathbf{0.6^{+0.5}_{-0.4} \pm 0.1}$ **(** $\mathbf{< 1.3}$**)**
$\boldsymbol{\eta'\pi^0}$	3663	$7.9^{+6.9}_{-5.2}$	1.2 ± 0.6	20.7	17.5	**1.4**	$\mathbf{0.8^{+0.8}_{-0.6} \pm 0.1}$ **(** $\mathbf{< 2.1}$**)**

resolutions in ΔE and $m_{\rm ES}$ with large control samples of B decays to charmed final states of similar topology (e.g. $B \to D(K\pi\pi)\pi$). For the combinatorial background the PDFs are determined in the fits to the data. However the functional forms are first deduced from fits of that component alone to sidebands in $(m_{\rm ES}, \Delta E)$, so that we can validate the fit before applying it to data containing the signal.

We use the following functional forms for the PDFs: sum of two Gaussians for $\mathcal{P}_{\rm sig}(m_{\rm ES})$, $\mathcal{P}_{{\rm sig},B\bar{B}}(\Delta E)$, and the sharper structures in $\mathcal{P}_{B\bar{B}}(m_{\rm ES})$ and $\mathcal{P}_j(m_k)$; linear or quadratic dependences for combinatorial components of $\mathcal{P}_{B\bar{B},q\bar{q}}(m_k)$ and for $\mathcal{P}_{q\bar{q}}(\Delta E)$; and a conjunction of two Gaussian segments below and above the peak with different widths, plus a broad Gaussian, for $\mathcal{P}_j(\mathcal{F})$. The $q\bar{q}$ background in $m_{\rm ES}$ is described by the function $x\sqrt{1-x^2}\exp[-\xi(1-x^2)]$, with $x \equiv 2{\rm m}_{\rm ES}/\sqrt{s}$ and parameter ξ. These are discussed in more detail in [1], and some of them are illustrated in Fig. 1.

We allow the parameters most important for the determination of the combinatorial background PDFs to vary in the fit, along with the yields for all components. Specifically, the free background parameters are most or all of the following, depending on the decay mode: ξ for $m_{\rm ES}$, linear and quadratic coefficients for ΔE, area and slope of the combinatorial component for m_k, and the mean, width, and width difference parameters for $\mathcal{F}$. Results for the yields are presented in the third column of Table II for each sample.

We test and calibrate the fitting procedure by applying it to ensembles of simulated $q\bar{q}$ experiments drawn from the PDF into which we have embedded the expected number of signal and $B\bar{B}$ background events randomly extracted from the fully simulated MC samples. We find biases of 0–2 events, somewhat dependent on the signal size. The bias values obtained for simulations that reproduce the yields found in the data are given in the fourth column of Table II.

In Fig. 1 we show, as representative of the several fits, the projections of the PDF and data for the $B^0 \to \eta'_{\eta\pi\pi}\pi^0$ sample. The goodness-of-fit is further demonstrated by the distribution of the likelihood ratio $\mathcal{L}_{\rm sig}/[\mathcal{L}_{\rm sig} + \sum \mathcal{L}_{\rm bkg}]$ for data and for simulation generated from the PDF model, shown for the same decay mode in Fig. 2. We see good agreement between the model and the data. By construction the background is concentrated near zero, while any signal would appear in a peak near one.

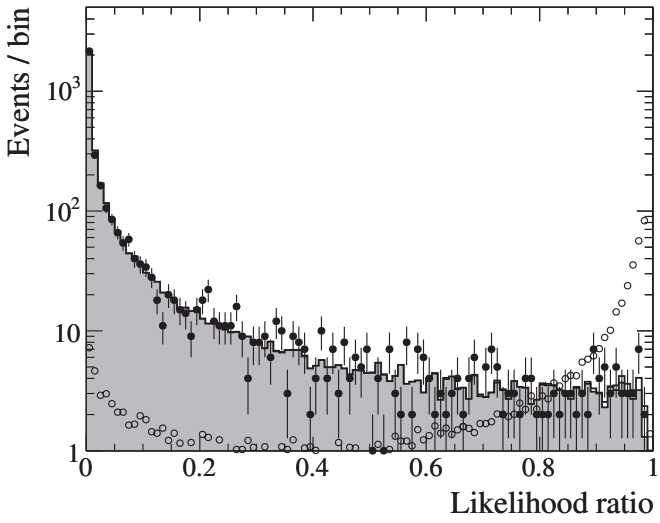

FIG. 2. The likelihood ratio $\mathcal{L}_{\rm sig}/[\mathcal{L}_{\rm sig} + \sum \mathcal{L}_{\rm bkg}]$ for $B^0 \to \eta'_{\eta\pi\pi}\pi^0$. The open circles represent a simulated signal component (normalized as the signal curves in Fig. 1), the solid points represent the data, the solid histograms are from samples of simulated background (shaded) and background plus signal (white, barely visible in the right-most bins, given the small signal yield).

We determine the reconstruction efficiencies, given in Table II, as the ratio of reconstructed and accepted events in simulation to the number generated. We compute the branching fraction for each channel by subtracting the fit bias from the measured yield, and dividing the result by the efficiency and the number of produced $B\bar{B}$ pairs [1]. We assume equal decay rates of the $\Upsilon(4S)$ to B^+B^- and $B^0\bar{B}^0$. Table II gives the numbers pertinent to these computations. The statistical error on the signal yield or branching fraction is taken as the change in the central value when the quantity $-2\ln\mathcal{L}$ increases by one unit from its minimum value.

We combine results where we have multiple decay channels by adding the functions $-2\ln\{[\mathcal{L}(\mathcal{B})/\mathcal{L}(\mathcal{B}_0)]\otimes G(\mathcal{B};0,\sigma')\}$, where $\mathcal{B}_0$ is the central value from the fit, σ' is the systematic uncertainty, and $\otimes G$ denotes convolution with a Gaussian function. We give the resulting final branching fractions for each mode in Table II with the significance, taken as the square root of the difference between the value of $-2\ln\mathcal{L}$ (with additive systematic uncertainties included) for zero signal and the value at its minimum. The 90% C.L. upper limits are taken to be the branching fraction below which lies 90% of the total of the likelihood integral in the positive branching fraction region.

The systematic uncertainties on the branching fractions arising from lack of knowledge of the PDFs have been included in part in the statistical error since most background parameters are free in the fit. For the signal, the uncertainties in PDF parameters are estimated from the consistency of fits to MC and data in control modes. Varying the signal-PDF parameters within these errors, we estimate yield uncertainties of 0–2 events, depending on the mode. The uncertainty from fit bias (Table II) includes its statistical uncertainty from the simulated experiments, and half of the correction itself, added in quadrature. Similarly we estimate the uncertainty from modeling the $B\bar{B}$ backgrounds by taking half of the contribution of that component to the fitted signal yield, 0.2–1.2 events. These additive systematic errors are dominant for these modes with little or no signal yield.

Uncertainties in our knowledge of the efficiency, found from auxiliary studies, include $0.8\% \times N_t$ and $1.5\% \times N_\gamma$, where N_t and N_γ are the number of tracks and photons, respectively, in the B candidate. The uncertainty in the total number of $B\bar{B}$ pairs in the data sample is 1.1%. Published data [17] provide the uncertainties in the B-daughter product branching fractions (0.7–3.9%). The uncertainties in the efficiency from the event selection are about 1%.

After combining the measurements we obtain the central values and 90% C.L. upper limits for the branching fractions:

$$\mathcal{B}(B^0\to\eta'\eta) = (0.2^{+0.7}_{-0.5}\pm 0.4)\times 10^{-6} (<1.7\times 10^{-6}),$$

$$\mathcal{B}(B^0\to\eta\pi^0) = (0.6^{+0.5}_{-0.4}\pm 0.1)\times 10^{-6} (<1.3\times 10^{-6}),$$

and

$$\mathcal{B}(B^0\to\eta'\pi^0) = (0.8^{+0.8}_{-0.6}\pm 0.1)\times 10^{-6} (<2.1\times 10^{-6}).$$

We find no evidence for these decays, and our upper limits represent two to three-fold improvement over the previous measurements [1,2,18]. The range of sensitivity of these measurements is comparable to the range of the theoretical estimates.

These results can be used to constrain the expected value of the CP asymmetry S_f in relation to $\sin 2\beta$ for the decay $B^0\to\eta' K^0$ [7,9,10]. Using the method proposed by Gronau *et al.* [10], we estimate that our results will provide approximately 20% improvement of the prediction for the contribution of the color-suppressed tree amplitude in $B^0\to\eta' K^0$ decays. This translates into a 20% reduction of this theoretical uncertainty in $S_{\eta' K^0_S}$. We find a similar improvement in the corresponding uncertainty of $\sin 2\alpha$ measured with $B^0\to\pi^+\pi^-$ decays [12,13].

We are grateful for the excellent luminosity and machine conditions provided by our PEP-II colleagues, and for the substantial dedicated effort from the computing organizations that support *BABAR*. The collaborating institutions wish to thank SLAC for its support and kind hospitality. This work is supported by DOE and NSF (USA), NSERC (Canada), IHEP (China), CEA and CNRS-IN2P3 (France), BMBF and DFG (Germany), INFN (Italy), FOM (The Netherlands), NFR (Norway), MIST (Russia), and PPARC (United Kingdom). Individuals have received support from CONACyT (Mexico), Marie Curie EIF (European Union), the A. P. Sloan Foundation, the Research Corporation, and the Alexander von Humboldt Foundation.

[1] B. Aubert *et al.* (*BABAR* Collaboration), Phys. Rev. D **70**, 032006 (2004).
[2] B. Aubert *et al.* (*BABAR* Collaboration), Phys. Rev. Lett. **93**, 181806 (2004).
[3] M. Beneke *et al.*, Nucl. Phys. **B591**, 313 (2000).
[4] M. Beneke and M. Neubert, Nucl. Phys. **B675**, 333 (2003).
[5] H. Wang *et al.*, Nucl. Phys. **B738**, 243 (2006).
[6] A. Williamson and J. Zupan, hep-ph/0601214.
[7] C. W. Chiang, M. Gronau, and J. L. Rosner, Phys. Rev. D **68**, 074012 (2003).

[8] C. W. Chiang, M. Gronau, and J. L. Rosner, Phys. Rev. D **70**, 034020 (2004).
[9] Y. Grossman *et al.*, Phys. Rev. D **68**, 015004 (2003).
[10] M. Gronau, J. L. Rosner, and J. Zupan, Phys. Lett. B **596**, 107 (2004).
[11] B. Aubert *et al.* (*BABAR* Collaboration), Phys. Rev. Lett. **94**, 161803 (2005); K. Abe *et al.* (Belle Collaboration), Phys. Rev. D **71**, 072003 (2005).
[12] M. Gronau and J. Zupan, Phys. Rev. D **71**, 074017 (2005).
[13] S. Gardner, Phys. Rev. D **72**, 034015 (2005).
[14] B. Aubert *et al.* (*BABAR* Collaboration), Nucl. Instrum. Methods Phys. Res., Sect. A **479**, 1 (2002).
[15] PEP-II Conceptual Design Report, SLAC Report No. R-418, 1993 (to be published).
[16] The *BABAR* detector Monte Carlo simulation is based on GEANT4: S. Agostinelli *et al.*, Nucl. Instrum. Methods Phys. Res., Sect. A **506**, 250 (2003).
[17] S. Eidelman *et al.* (Particle Data Group), Phys. Lett. B **592**, 1 (2004).
[18] P. Chang *et al.*, Phys. Rev. D **71**, 091106 (2005).